

Burn-induced subepicardial injury in frog heart: a simple model mimicking ST segment changes in ischemic heart disease

Itsuro KAZAMA^{1)*}

¹⁾Department of Physiology I, Tohoku University Graduate School of Medicine, Seiryō-cho, Aoba-ku, Sendai, Miyagi 980–8575, Japan

(Received 27 July 2015/Accepted 26 August 2015/Published online in J-STAGE 7 September 2015)

ABSTRACT. To mimic ischemic heart disease in humans, several animal models have been created, mainly in rodents by surgically ligating their coronary arteries. In the present study, by simply inducing burn injuries on the bullfrog heart, we reproduced abnormal ST segment changes in the electrocardiogram (ECG), mimicking those observed in ischemic heart disease, such as acute myocardial infarction and angina pectoris. The “currents of injury” created by a voltage gradient between the intact and damaged areas of the myocardium, negatively deflected the ECG vector during the diastolic phase, making the ST segment appear elevated during the systolic phase. This frog model of heart injury would be suitable to explain the mechanisms of ST segment changes observed in ischemic heart disease.

KEY WORDS: bullfrog heart, burn injury, currents of injury, ischemic heart disease, ST segment change

doi: 10.1292/jvms.15-0440; *J. Vet. Med. Sci.* 78(2): 313–316, 2016

Ischemic heart disease, including myocardial infarction and angina pectoris, is a leading cause of morbidity and mortality in the world [8]. The large loss of cardiomyocytes induced by ischemia often leads to an impairment of the cardiac contractility, loss of pump function and subsequent onset of heart failure [11]. The disease also provokes serious ventricular tachyarrhythmia, occasionally causing sudden cardiac death [1]. To mimic myocardial infarction in humans, several animal models have been created in rodents (mice and rats) or other mammals (rabbits, dogs and pigs) [16]. The procedure includes surgical ligation, cauterization or cryo-injury of the left anterior descending coronary arteries (LAD) to induce myocardial ischemic damage [9, 12, 16]. However, due to the increased cost of such animals and specific instruments required for the procedure, including respiratory machines and anesthesia apparatuses, the use of these models was often limited to highly specialized laboratories [14]. Using the isolated hearts from bullfrogs, previous studies revealed the electrophysiological properties of cardiac muscles together with their mechanisms [2, 15]. In these studies, the electrocardiogram (ECG) recorded from the frog heart showed an almost identical pattern to that of humans or rodents [15], indicating its usefulness as a mimic of the human heart. Therefore, the purpose of our study was to establish a simple model of myocardial damage in frog hearts. Here, by simply inducing burn injuries on the bullfrog heart, we reproduced ECG abnormalities representing those observed in ischemic heart disease, such as acute

myocardial infarction and angina pectoris. Using this model, we will also explain the mechanisms of ST segment changes observed in human ischemic heart diseases.

Adult male bullfrogs weighing 400–500 g ($n=22$), purchased from Mr. Ohuchi Kazuo, were initially anesthetized by diethyl-ether, which was inhaled only a short period of time as an inductive anesthesia. The frogs were then subjected to the intramuscular injection of a long-acting anesthetic, ethyl carbamate (0.50 g/kg; Wako Pure Chemical Industries, Ltd., Osaka, Japan), which was effective through the experiment. After deeply anesthetized, the frogs were placed on plates in the supine position. As previously described [15], the thorax was opened with a pair of scissors for the skin and muscles, and another pair of bone scissors for thoracotomy. The covering pericardium was removed with forceps to expose the heart. An ECG was used to record electrical signals from the bullfrog heart. A silver wire, which was coated with a layer of silver chloride and soldered to the output pin, was gently placed on the surface of the ventricle (the positive pole) and connected to the ECG amplifier, which was of our own making as previously recommended [15]. Wilson’s central terminal, which is obtained by averaging the measurements from the electrodes from the right arm, left arm and the left foot, was used as the negative pole. This represented a pericardial lead detected directly from the ventricular surface instead of the thoracic surface. The ECG waveforms were detected by an oscilloscope (TDS 1002, Tektronix Inc., Beaverton, OR, U.S.A.) connected to a monitor (Thermal array recorder Type WR310, GRAPHTEC Corp., Yokohama, Japan). To record the transmembrane potential, the suction-electrode method was employed as originally described by Irisawa *et al.* [5]. A chloride-coated silver wire, inserted into a polyethylene tube (–1 mm in diameter), was placed on the surface of the ventricle and connected to the amplifier. The inside of the tube was filled with external solution containing (in mM): NaCl, 115; KCl, 2; CaCl₂, 2.0; MgCl₂, 1.0; Hepes, 5.0; and Na-Hepes 5.0 (pH 7.4 adjusted with NaOH). Using a syringe

*CORRESPONDENCE TO: KAZAMA, I., Department of Physiology I, Tohoku University Graduate School of Medicine, Seiryō-cho, Aoba-ku, Sendai, Miyagi 980–8575, Japan.
e-mail: kazaitu@med.tohoku.ac.jp

©2016 The Japanese Society of Veterinary Science

This is an open-access article distributed under the terms of the Creative Commons Attribution Non-Commercial No Derivatives (by-nc-nd) License <<http://creativecommons.org/licenses/by-nc-nd/3.0/>>.

connected to the tube, a negative pressure was applied to the recording electrode to break the cellular membranes under the tube. All experimental protocols described in the present study were approved by the Ethics Review Committee for Animal Experimentation of Tohoku University.

By simultaneously applying the ECG recording and the suction-electrode techniques to the heart muscle, we obtained electrical traces from the middle portion of the ventricle, as shown in Fig. 1. The top trace shows the ECG with the prominent QRS complexes, although the P and T waves, which indicate the atrial depolarization and ventricular repolarization, respectively [15], are almost indecipherable. The bottom trace illustrates the action potential of the ventricular cardiomyocytes, which consists of five phases including “rapid upstroke (phase 0)”, “partial repolarization (phase 1)”, “plateau (phase 2)”, “rapid repolarization (phase 3)” and “resting membrane potential (phase 4)”. As previously shown in frog hearts [15], the QRS complex and the following wave (possibly T wave) synchronized with the rapid upstroke (phase 0) and rapid repolarization (phase 3) of the action potential, indicating that the QRS complex and the following T wave respectively reflected the excitation and de-excitation processes of the ventricular cardiomyocytes.

To induce subepicardial injury, the tip of a glass capillary tube with a diameter of 1.5 mm was heated in the flame to more than 600°C and gently applied to the ventricular wall of the heart (Fig. 2A). By repeatedly imposing the heated tube for a few sec, several overlapping burn injuries, with diameters of approximately 2–4 mm, were made in the subepicardial myocardium adjacent to the ventricular surface where the ECG recording electrode was placed (Fig. 2A). The trial numbers of the injuries were decided to mimic the minimum size of myocardial infarction in rodent models, which was induced by the coronary artery ligation [14]. Before the injuries were made, the ECG showed normal QRS complexes followed by positive T waves (Fig. 2B top), between which were the ST and TQ segments recorded on the isoelectric line (Fig. 2B top). However, immediately after the burn injuries were made, the ECG demonstrated a prominent elevation of the ST segment (17.6 ± 3.4 mV, $n=5$), which was far above the isoelectric baseline (Fig. 2B bottom), indicating the induction of myocardial injury. The mechanisms by which the subepicardial burn injury induced the ST segment elevation can be explained as follows (Fig. 3A). Due to the cellular damage, the extracellular concentration of K^+ ions is elevated around the injured cells (Fig. 3Aa) [10], which makes their resting membrane potential significantly higher than that of the adjacent intact cells (Fig. 3Ab). This difference creates a voltage gradient between the intact and damaged areas of the myocardium during the diastolic phase of the cardiac cycle, producing “currents of injury” (Fig. 3Ac), which arise from the damaged subepicardium and flow towards the intact endocardium [6]. Since the currents flow away from the ECG recording electrode placed adjacent to the burn injury (Fig. 3Ac), the ECG vector during the diastolic phase shows a negative deflection from the isoelectric line (Fig. 3Ad), making the ST segment appear elevated during the systolic phase.

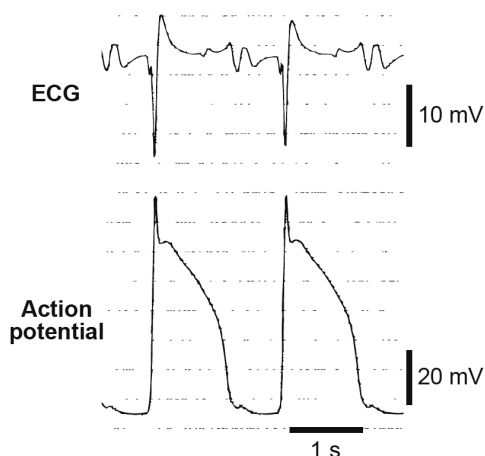


Fig. 1. Simultaneous recordings of the electrocardiogram (ECG) and the transmembrane action potential in the bullfrog heart. The top trace shows the ECG with the prominent QRS complexes, although the P and T waves are almost indecipherable. The bottom trace illustrates the action potential of ventricular cardiomyocytes, which consists of five phases including phase 0 (rapid upstroke), 1 (partial repolarization), 2 (plateau), 3 (rapid repolarization) and 4 (resting membrane potential).

In human ischemic heart diseases, such as acute myocardial infarction and angina pectoris, hypoxic cellular damage leads to the diminished intracellular concentration of adenosine triphosphate (ATP). Such loss of ATP decreases the activity of the ATP-dependent transport system, including Na^+/K^+ -ATPase, which normally transports K^+ ions into the cell, but Na^+ ions out of the cell [3]. As a result of the decreased pump activity, K^+ ions are prevented from being pumped back into the cells, which decreases their intracellular concentration, but increases their extracellular concentration instead. This also creates the difference in the resting membrane potential between the intact and ischemic areas of the myocardium (Fig. 3Ab) and produces the “currents of injury” as were the cases with the burn-induced cardiac injury in frogs (Fig. 3Ac).

In cases of acute myocardial infarction, since severe ischemia usually induces transmural myocardial damage (Fig. 3Ba), the “currents of injury” flow away from the ECG recording electrode (pericardial lead), which is placed on the same side of the injured ventricular wall (Fig. 3Ba) [6]. Therefore, as was the case with the subepicardial burn injury in our experiment (Fig. 3Ad), the ECG changes observed in myocardial infarction are primarily featured by an elevation of the ST segment during the acute phase [13]. On the other hand, in cases of angina pectoris, myocardial injuries are frequently induced in the subendocardial areas (Fig. 3Bb), which are anatomically most prone to the oxygen deprivation [13]. Therefore, in such cases, the “currents of injury” that arise from the subendocardium flow towards the intact ventricular surface where the pericardial lead is placed (Fig. 3Bb) [4]. The direction of the currents is opposite of that in myocardial infarction (Fig. 3Ba) or the burn injury in our experiment (Fig. 3Ac). This causes the ECG vector

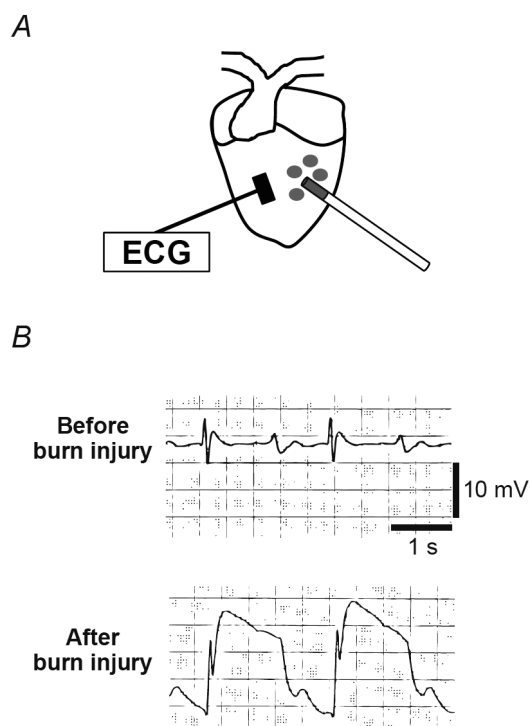


Fig. 2. Induction of subepicardial burn injury and the ECG changes in the bull frog heart. (A) To induce subepicardial burn injuries, a heated glass capillary tube was repeatedly imposed on the ventricular wall adjacent to where the ECG recording electrode was placed. (B) ECG changes before (top) and after the injuries (bottom).

in angina pectoris to show positive deflection during the diastolic phase, making the ST segment appear depressed during the systolic phase [13]. Additionally, differing from a simple burn injury, the cardiac ischemia also facilitates the opening of K_{ATP} -channels during the systolic phase [7], which accelerates the rapid repolarization (phase 3) of the action potential, significantly shortening its duration. This also creates a voltage gradient between the intact and anorexic areas during the systolic phase, producing currents that flow against the “currents of injury”. Since such currents positively or negatively deflect the ECG vectors during the systolic phase, they would have additional effects on the ST segment changes observed in ischemic heart disease.

In conclusion, using the bullfrog heart, we introduced a simple model representing the ST segment changes in ischemic heart disease, such as acute myocardial infarction and angina pectoris. This frog model of heart injury would be suitable to explain the mechanisms of ST segment changes observed in ischemic heart disease.

REFERENCES

1. Bailey, J. J., Berson, A. S., Handelsman, H. and Hodges, M. 2001. Utility of current risk stratification tests for predicting major arrhythmic events after myocardial infarction. *J. Am. Coll.*

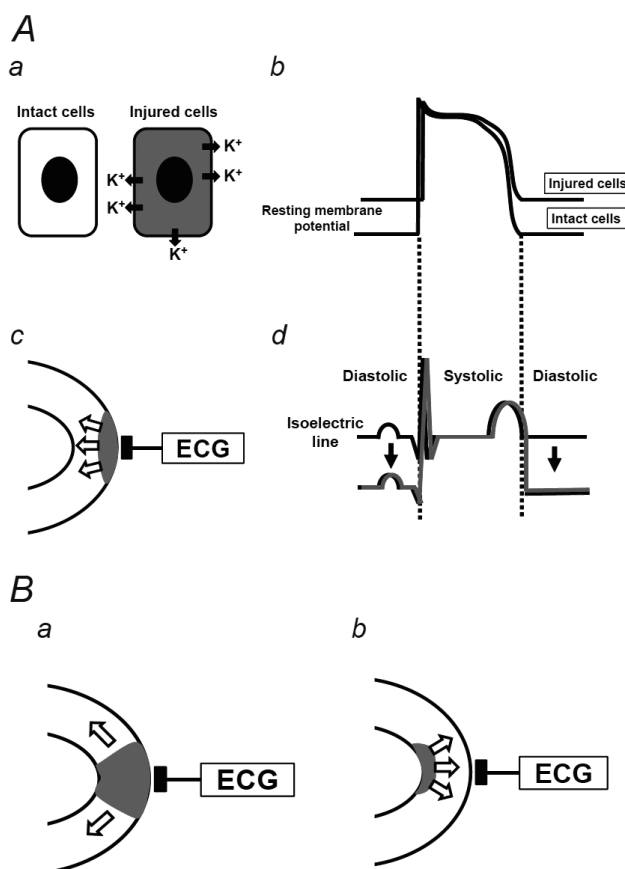


Fig. 3. Mechanisms of ST segment changes in subepicardial burn injury and ischemic heart disease. (A) Mechanisms of ST segment elevation in subepicardial burn injury. The extracellular concentration of K^+ ions is elevated around the injured cardiomyocytes (a), which makes their resting membrane potentials significantly higher than those of adjacent intact cells (b). Such difference creates a voltage gradient between the intact and damaged areas of the myocardium during the diastolic phase of the cardiac cycle (b), producing “currents of injury” (white arrows), which arise from the damaged subepicardium and flow towards the intact endocardium. Since the currents flow away from the ECG recording electrode placed adjacent to the burn injury (c), the ECG vector during the diastolic phase shows a negative deflection from the isoelectric line (d, arrows), making the ST segment appear elevated during the systolic phase (d, gray waveform). (B) Directions of the “currents of injury” (white arrows) in ischemic heart disease, such as acute myocardial infarction (a) and angina pectoris (b). a: In acute myocardial infarction, the currents flow away from the ECG recording electrode (pericordial lead) towards the other side of the intact ventricle wall. b: In angina pectoris, the currents arise from the damaged endocardium and flow towards the intact ventricular surface where the ECG recording electrode is placed.

Cardiol. 38: 1902–1911. [Medline] [CrossRef]

2. Fasciano, R. W. 2nd. and Tung, L. 1999. Factors governing mechanical stimulation in frog hearts. *Am. J. Physiol.* 277: H2311–H2320. [Medline]
3. Fuller, W., Parmar, V., Eaton, P., Bell, J. R. and Shattock, M. J. 2003. Cardiac ischemia causes inhibition of the Na/K ATPase by a labile cytosolic compound whose production is linked to

- oxidant stress. *Cardiovasc. Res.* **57**: 1044–1051. [[Medline](#)] [[CrossRef](#)]
4. Gingham, C., Ungureanu, C., Vladaia, A., Popescu, B. A. and Jurcut, R. 2009. The electrocardiographic profile of patients with angina pectoris. *J. Med. Life* **2**: 80–91. [[Medline](#)]
 5. Irisawa, H. and Kobayashi, M. 1964. On the spontaneous activities of oyster myocardium caused by several inorganic ions in sucrose solution. *Jpn. J. Physiol.* **14**: 165–176. [[Medline](#)] [[CrossRef](#)]
 6. Kléber, A. G. 2000. ST-segment elevation in the electrocardiogram: a sign of myocardial ischemia. *Cardiovasc. Res.* **45**: 111–118. [[Medline](#)] [[CrossRef](#)]
 7. Lascano, E. C., Negroni, J. A. and del Valle, H. F. 2002. Ischemic shortening of action potential duration as a result of KATP channel opening attenuates myocardial stunning by reducing calcium influx. *Mol. Cell. Biochem.* **236**: 53–61. [[Medline](#)] [[CrossRef](#)]
 8. Lloyd-Jones, D. M., Larson, M. G., Beiser, A. and Levy, D. 1999. Lifetime risk of developing coronary heart disease. *Lancet* **353**: 89–92. [[Medline](#)] [[CrossRef](#)]
 9. Munz, M. R., Faria, M. A., Monteiro, J. R., Aguas, A. P. and Amorim, M. J. 2011. Surgical porcine myocardial infarction model through permanent coronary occlusion. *Comp. Med.* **61**: 445–452. [[Medline](#)]
 10. Page, E. 1962. The electrical potential difference across the cell membrane of heart muscle. Biophysical considerations. *Circulation* **26**: 582–595. [[Medline](#)] [[CrossRef](#)]
 11. Pfeffer, J. M., Pfeffer, M. A., Fletcher, P. J. and Braunwald, E. 1991. Progressive ventricular remodeling in rat with myocardial infarction. *Am. J. Physiol.* **260**: H1406–H1414. [[Medline](#)]
 12. Pfeffer, M. A., Pfeffer, J. M., Fishbein, M. C., Fletcher, P. J., Spadaro, J., Kloner, R. A. and Braunwald, E. 1979. Myocardial infarct size and ventricular function in rats. *Circ. Res.* **44**: 503–512. [[Medline](#)] [[CrossRef](#)]
 13. Wagner, G. S., Macfarlane, P., Wellens, H., Josephson, M., Gorgels, A., Mirvis, D. M., Pahlm, O., Surawicz, B., Kligfield, P., Childers, R., Gettes, L. S., Bailey, J. J., Deal, B. J., Gorgels, A., Hancock, E. W., Kors, J. A., Mason, J. W., Okin, P., Rautaharju, P. M., van Herpen G., American Heart Association Electrocardiography and Arrhythmias Committee, Council on Clinical Cardiology American College of Cardiology Foundation Heart Rhythm Society Endorsed by the International Society for Computerized Electrocardiology. 2009. AHA/ACCF/HRS recommendations for the standardization and interpretation of the electrocardiogram: part VI: acute ischemia/infarction: a scientific statement from the American Heart Association Electrocardiography and Arrhythmias Committee, Council on Clinical Cardiology; the American College of Cardiology Foundation; and the Heart Rhythm Society. *J. Am. Coll. Cardiol.* **53**: 1003–1011. [[Medline](#)] [[CrossRef](#)]
 14. Wang, J., Bo, H., Meng, X., Wu, Y., Bao, Y. and Li, Y. 2006. A simple and fast experimental model of myocardial infarction in the mouse. *Tex. Heart Inst. J.* **33**: 290–293. [[Medline](#)]
 15. Yoshida, S. 2001. Simple techniques suitable for student use to record action potentials from the frog heart. *Adv. Physiol. Educ.* **25**: 176–186. [[Medline](#)]
 16. Zaragoza, C., Gomez-Guerrero, C., Martin-Ventura, J. L., Blanco-Colio, L., Lavin, B., Mallavia, B., Tarin, C., Mas, S., Ortiz, A. and Egido, J. 2011. Animal models of cardiovascular diseases. *J. Biomed. Biotechnol.* **2011**: 497841. [[Medline](#)] [[CrossRef](#)]